Temperature-Responsive and Passive Wireless Mechanical Metamaterial Sensors

VISHNU R. NAIDU, YUJIN PARK and KENNETH J. LOH

ABSTRACT

Knowing the location and environmental conditions of sailors that have fallen overboard can greatly facilitate open water search and rescue operations. Currently, active sensors that trigger an alarm when a sailor falls overboard exist, and it works by detecting a loss of signal from a transmitter. However, their applications have been limited because of the dependence on a working battery, as well as the fact that sailor location cannot be tracked beyond the one-time loss-of-signal event. In this study, a passive, person-overboard sensing concept is proposed, and the focus is to demonstrate monitoring of seawater conditions. The passive sensor was designed by incorporating a temperature-responsive hydrogel with an auxetic star pattern unit cell geometry, which transforms from a two- to three-dimensional geometry when immersed in low temperature liquid. First, the passive sensor was formed by incorporating a temperature-responsive hydrogel at opposite ends of the star pattern. The time-dependent swelling and de-swelling behavior of the copolymer hydrogel was characterized to understand the mechanical strains induced after exposure to low temperature water. Second, the design of the star pattern geometry was optimized, and artificial imperfections in the form of notches were employed to allow shape transformation to take place at appropriate and minimal applied strains. The vision is that these shape morphing structures with integrated antennas can serve as passive sensors, which, when interrogated by a remote reader, can be used to monitor how long overboard sailors have been in a low-temperature open sea environment.

INTRODUCTION

Search and rescue operations at sea due to a person-overboard event are presently hampered by the lack of information such as sailor identification, time of event, water

Vishnu Naidu[1], Yujin Park[1], and Kenneth J. Loh[1,2,*]
[1]Materials Science and Engineering Program, University of California San Diego, La Jolla, CA 92093, USA
[2]Department of Structural Engineering, University of California San Diego, La Jolla, CA, 92093 USA * E-mail: kenloh@ucsd.edu

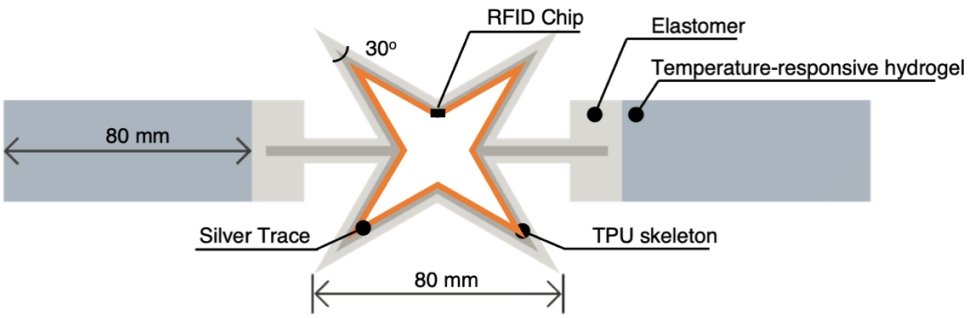

Figure 1. The passive wireless mechanical metamaterial sensor with temperature-responsive hydrogels at opposite ends of the star pattern is shown.

temperature, and location of event. Current person-overboard detection systems employ fixed camera-based and/or scanning technologies, active continuously monitored personal devices (*e.g.*, wristbands and fobs), and active wearables (*e.g.*, safety vests). Fixed systems need to be pre-installed in areas of interest on the ship, while active personal devices and wearables rely on working batteries and need to be always worn or carried to be effective. Person-overboard detection systems can provide limited information about the person-overboard event, such as identification and location, but usually not more than that. Therefore, a passive always-worn sensor that can provide identification, event location and seawater conditions can be highly advantageous for directing and prioritizing search and rescue operations.

The goal of this study is to develop a passive sensor that can be worn as a wearable patch, which can be remotely interrogated to obtain the aforementioned information following a person-overboard event. The passive sensor leverages the concept of a Bio-inspired Active Skin (BIAS), wherein two-dimensional (2D) patterns with a printed conductive trace antenna can morph into three-dimensional (3D) structures upon the application of in-plane strains [1]. The 2D structure in this case is an elastomeric auxetic star unit cell pattern, with a temperature-responsive hydrogel actuator on both ends (Figure 1). In-plane strain is generated by the deswelling behavior of the bookended temperature-responsive hydrogels. This design results in a structure that can shape morph in response to changing temperature, which would in turn modify its antenna signature as measured by a remote wireless reader. The vision is that this shape morphing passive patch sensor, when always worn by sailors as part of their uniforms, will facilitate their search and rescue during an emergency.

HYDROGEL BACKGROUND

Hydrogels are a group of materials that are capable of swelling (by imbibing large amounts of water) and de-swelling (by expelling large amounts of water) while retaining their basic shape due to chemical (or physical) cross-linking. The hydrogels used in this study were chemically cross-linked by reactions between selected chemical groups and were formulated to reversibly swell and de-swell when exposed to varying water temperatures, thus rendering them temperature sensitive.

The variable of particular interest in temperature sensitive hydrogels is the lower critical solution temperature (LCST). This is the temperature below which the

hydrogel is predominantly hydrophilic and above which the hydrogel is predominantly hydrophobic. While typical hydrogels exhibit an LCST of around 32 °C [2], the N-tert-butyl acrylamide (NTBAM)-N-isopropyl acrylamide (NIPAM)-acrylamide (AM) copolymer hydrogels were formulated for LCST values of between about 8 °C and 10 °C, as demonstrated by Tang *et al.* [2]. The NTBAM-NIPAM-AM copolymer hydrogels that were formulated for this study were designed to swell and de-swell at temperatures below and above the LCST, respectively.

To actuate the antenna using an NTBAM-NIPAM-AM copolymer hydrogel, a non-responsive passive elastomer that can form bonds with the hydrogel is required. Polydimethylsiloxane (PDMS) is a commonly used elastomer; however, due to its hydrophobicity, it cannot naturally form bonds with hydrophilic hydrogels [3]. Nevertheless, various surface modification methods such as oxygen plasma treatment [4] or the use of photo-initiators [5] can induce free-radical reactions between PDMS and monomers. Therefore, in this study, a simple mixture of benzophenone and PDMS was used to enable UV-mediated free radical polymerization on the PDMS surface while maintaining the integrity of the hydrogel.

EXPERIMENTAL DETAILS

Two types of experiments were conducted, one with the temperature-responsive hydrogels and another with the star pattern and integrated antenna. The hydrogel experiments were performed to assess the amount of actuation that the hydrogel can be expected to impart to the shape morphing geometry. The star pattern and integrated antenna experiments were done to optimize its shape morphing responsiveness.

Fabrication of Temperature-responsive Hydrogels

Two sets of hydrogels, namely sample set 1 and sample set 2, were fabricated by varying the amount of solvent and cross-linking agent in each set. Each sample set contained three samples. The samples were synthesized by combining three monomers, namely NTBAM (0.525 mmol/mL), NIPAM (0.150 mmol/mL) and AM (0.25 mmol/mL), with two solvents, namely deionized water (4.5 mL for sample set 1 and 1.5 mL for sample set 2) and tert-butanol (7.5 mL for each sample set), and a cross-linking agent, N-N'methylenebisacrylamide (MBA) (3 mL solution for sample set 1 and 6 mL solution for sample set 2), in general accordance with Tang *et al.* [2]. The MBA solution concentration was 1.80 mg/mL for sample set 1 and 3.6 mg/mL for sample set 2. The 15 mL solution of each sample set was mixed in a FlackTek speed mixer and heated to 60 °C. Potassium persulfate (KPS) (150 µL) was then added as an initiating agent, and the solution was once again mixed in a FlackTek speed mixer. Following this, 5 mL of solution was pipetted out into each of three cylindrical polypropylene laboratory containers. The six containers were then placed in a vacuum oven at 60 °C for 12 h to allow the samples to cure. Each cured sample resembled a roughly ∅25 mm disc with a nominal thickness of 6 mm. After curing, the hydrogel samples were rinsed in deionized water to remove any unreacted monomers and then placed in fresh deionized water in a refrigerator at approximately 4 °C for a minimum of 24 h, in order to allow equilibrium swelling of the samples.

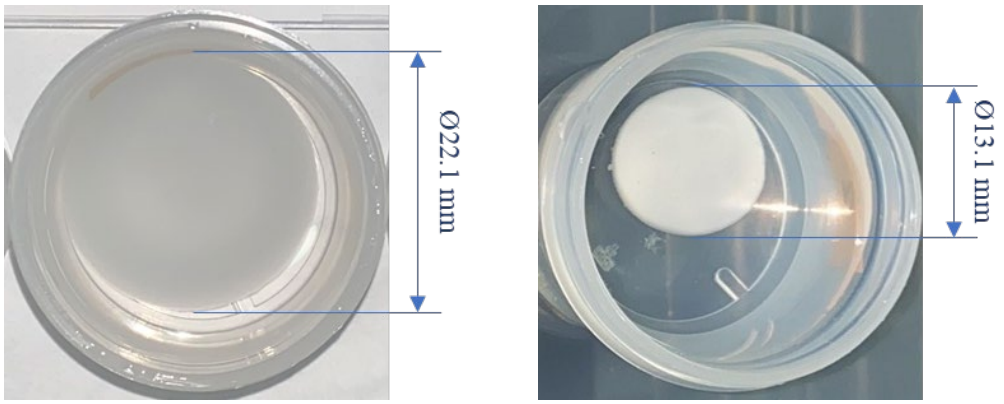

(a) (b)

Figure 2. (a) A hydrogel sample is shown fully swelled after soaking for more than 24 h in ~ 4 °C water. (b) The same sample is shown after de-swelling for 20 min in 15 °C water.

Hydrogel Deswelling Behavior

The two different hydrogel sample sets were placed in deionized water at six test temperature regimes, namely, 4, 6, 8, 13, 15, and 22 °C for 20 min. For each test temperature, the average diameters of the discs were reported for both sample sets via simple photogrammetry from the time of immediate exposure to each test temperature for a total exposure time of 20 min in 2 min increments (see Figure 2).

Fabrication of Tensile Test Samples and Testing Protocol

A tensile test sample was prepared following ASTM D638 type IV to obtain hyperelastic material parameters for PDMS, which can be used in finite element simulations, since the BIAS star geometry for the passive antenna was created using PDMS. The PDMS base material was prepared by adding 1.8 wt% benzophenone to reduce their hydrophobicity. The benzophenone, which is solid at room temperature, was liquefied at around 80 °C before being added to the PDMS and then mixed using a Flacktek speed mixer at 3,000 rpm for 2 min. Afterwards, 5 wt% PDMS cross-linker was added and mixed for 5 min at 1,000 rpm to prepare the PDMS prepolymer. The prepared prepolymer was transferred into a syringe, then centrifuged at 3,000 rpm for 20 min to remove all air, before being used for casting. The casting mold for each tensile specimen and BIAS star geometry was designed using *Fusion 360* and then 3D-printed using thermoplastic urethane (TPU) using an Ultimaker *3+* fused deposition modeling printer. A layer of petrolatum was applied to the mold to prevent the cured PDMS from sticking to the mold for ease of demolding. The PDMS prepolymer was then deposited in the mold and cured at 80 °C for 1 h. Each PDMS tensile coupon was subjected to uniaxial tension using a Test Resource 150R load frame. The testing rate was set at 1 mm/s, and the test continued until the specimen fractured.

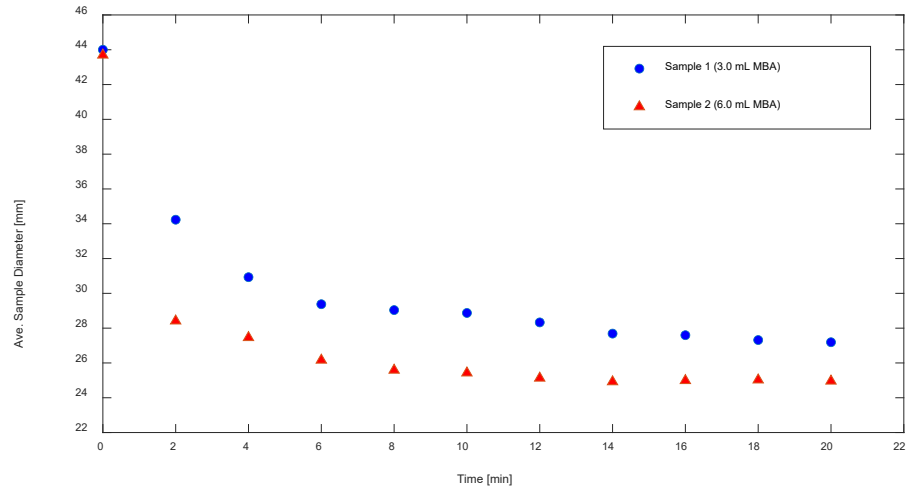

Figure 3. The average sample diameter data versus time is shown for both test sample sets at 15 °C during a 20 min exposure time in deionized water.

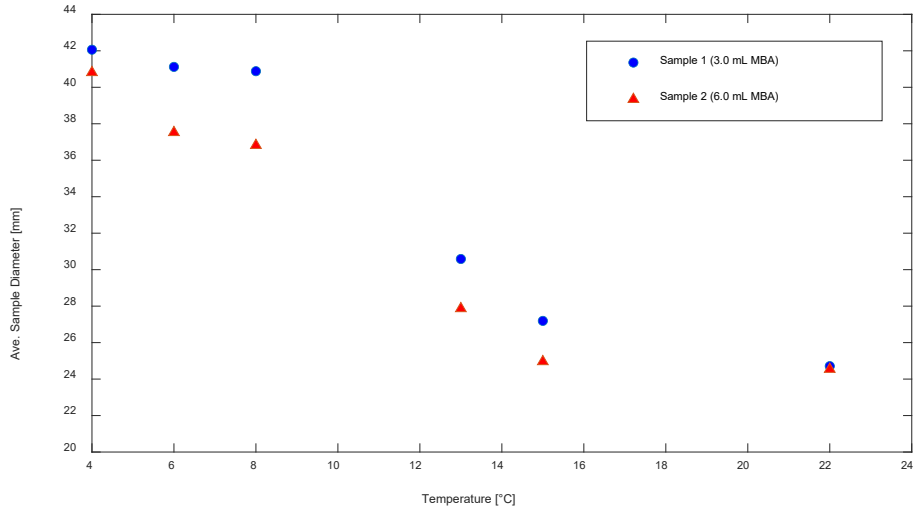

Figure 4. The average sample diameter data for the six temperature regimes at a time slice of 20 min is shown.

RESULTS AND DISCUSSION

Deswelling Behavior of Low Temperature-Responsive Hydrogel

The synthesized temperature-sensitive hydrogel samples were tested to obtain de-swelling data, which would then be used to actuate the shape morphing BIAS pattern and its integrated antenna. Figures 3 and 4 show the results obtained. Each of the two sample sets was exposed to deionized water at 4, 6, 8, 13, 15, and 22 °C for 20 min. Figure 3 shows how the diameters of the two different hydrogel sample sets changed during the 15 °C test. The diameter versus time data plots for the 4, 6, 8, 13, and 22 °C tests followed the same general pattern as that for the 15 °C shown in Figure

TABLE I. MOONEY-RIVLIN PARAMETERS OF PDMS

C_{10} [MPa]	C_{01} [MPa]	C_{11} [MPa]	C_{20} [MPa]	C_{02} [MPa]	P [kg/m^3]
0.023	0.035	-0.149	0.047	0.142	965

3. The plots showed a sharp decrease in diameter within approximately 8 to 10 min and then stabilized to a more-or-less constant value from then onwards.

The LCST was estimated, from Figure 4 to be between 8 and 15 °C. The percentage decrease in diameter for each of the two sample sets after 20 min at the two temperatures that were ostensibly above the LCST was 38% for sample set 1 and 42% for sample set at 15 °C, and 43% for both sample sets at 22 °C. With one hydrogel actuator on each end of the auxetic star pattern, both hydrogel actuators would be easily capable of imposing a 50% strain on the BIAS star pattern when exposed to water.

Numerical Modeling

Experimentally calibrated finite element (FE) simulations using *COMSOL Multiphysic*s were created to determine the optimal width of the BIAS geometry for inducing 3D deformations. However, properties of the PDMS substrate were needed to define the *COMSOL* hyperelastic numerical model. Therefore, the tensile test load-displacement data of PDMS was converted to stress-stretch and fitted using nonlinear least-square regression to obtain the five Mooney-Rivlin parameters. The first Piola-Kirchoff stress can be expressed below, assuming the material is incompressible.

$$P=2(1-\lambda^{-3})(\lambda C_{10}+2C_{20}\lambda(I_{1_{\text{uni}}}-3)+C_{11}\lambda(I_{2_{\text{uni}}}-3)+C_{01}+2C_{02}(I_{2_{\text{uni}}}-3)+C_{11}(I_{1_{\text{uni}}}-3)) \quad (1)$$

The five Mooney-Rivlin parameters are listed in Table I and were used for parametric optimization in *COMSOL Multiphysics*. One end of the BIAS star geometry was fixed, and uniaxial tension was applied to the opposite end to induce a 50% strain in the star geometry. The load-displacement behavior of each geometry was captured during this process.

Geometric Optimization

FE simulations were performed to identify the optimal width (w) that promoted 3D deformations or shape morphing of the BIAS star geometry. Figure 5 shows the top and side views of both the pristine and deformed states of a BIAS star geometry, along with the dimensions used in the FE model. The outer tip spacing (D), rib angle, and thickness were fixed at 80 mm, 30°, and 3 mm, respectively. The 30° rib angle was previously determined as optimal [6]. When uniaxial strain was applied to the BIAS star geometry, localized compression was induced on the beam between the inner and outer tips. Buckling occurred when this compression exceeded the critical buckling force of the beam. When the width was greater than the thickness, buckling occurred in the out-of-plane direction, allowing for 3D deformations to occur. Previous research also showed that, when the length of the notch applied to the beam exceeded 50% (blue shaded region

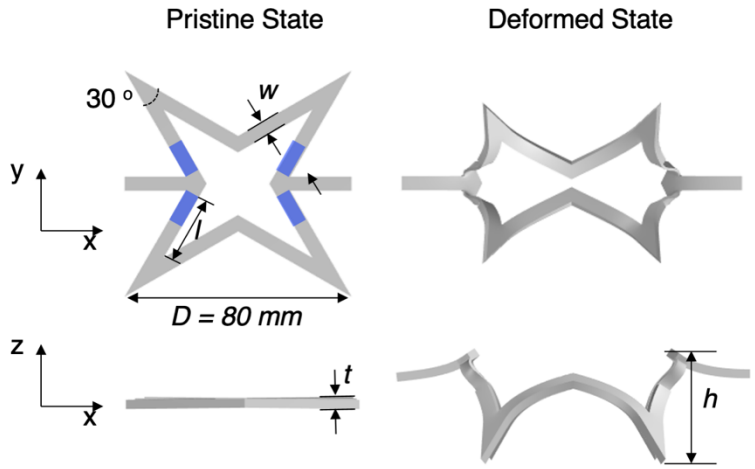

Figure 5. The top and side views of the BIAS star geometry are shown in its pristine and deformed states, along with the corresponding dimensions for the finite element simulations.

in Figure 5), it was possible to control buckling orientation in the opposite direction (downwards in Figure 5) of the indented surface. Therefore, in this study, notches with a length of 50% of the beam's length and a depth of 2/3 of the thickness were always created, followed by parametric optimization with respect to *w*.

The out-of-plane buckling instability of the BIAS star geometry was inversely proportional to *w*. When the BIAS star geometry was stretched, the outer and inner tips move in the out-of-plane direction. The distance between these tips is referred to as *h* (see Figure 5). As it strained, *h* gradually increased, reached a maximum, and then decreased again. The point of reaching the maximum value is known as full deployment. Figure 6(a) displays the strain and stress required for BIAS star geometry to reach full deployment. Geometries with *w* = 3 and 4 mm did not reach full deployment at 50% strain. However, geometries with *w* = 5 to 7 mm reached full deployment within 40% strain. The required strain decreased as *w* increased, while BIAS star geometries with a wider *w* required greater forces because of their higher stiffness. In addition, Figure 6(b) illustrates the deployment of BIAS geometries with *w* = 4 and 6 mm as a function of strain. BIAS with a wider *w* achieved full deployment and experienced out-of-plane

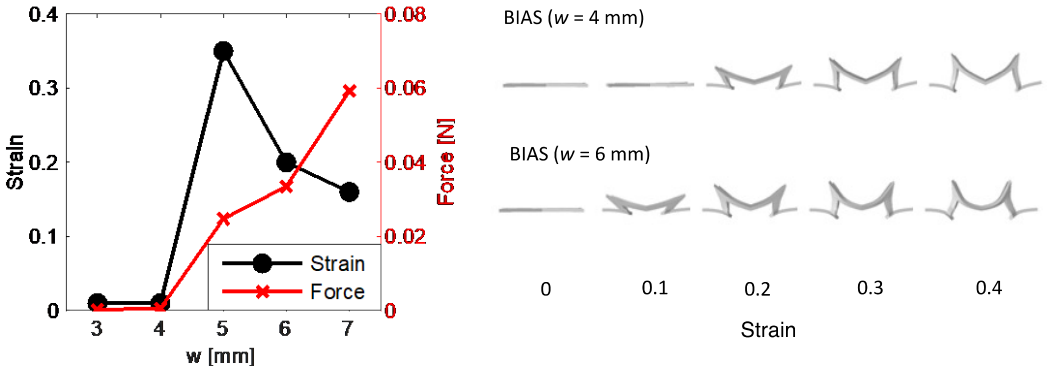

(a) (b)

Figure 6. Forces and strains were determined at full deployment of the BIAS star geometry for various widths.

deformation at a lower strain. Although all BIAS star geometries with w ranging from 5 to 7 mm shape morphed at below 40% strain, the geometry with w = 6 mm, which demanded relatively lower strain and force, was identified as the most optimal geometry for the antenna.

CONCLUSIONS

The overarching goal of this research is that shape morphing structures with integrated antennas can serve as passive sensors, which, when interrogated by a remote reader, can be used to monitor how long overboard sailors have been in a low-temperature open sea environment. In this work, the objective was to demonstrate that an auxetic star pattern structure, when subjected to strains induced by temperature responsive hydrogels, could shape morph by exhibiting out-of-plane deformations. The temperature sensitive hydrogel that was incorporated with the elastomer star unit cell pattern had an LCST of between 8 and 15 °C. When exposed to cold water, the experiments confirmed that the hydrogels de-swelled to induce strains on the star pattern to cause shape morphing. In addition, numerical simulations of the star geometry were performed to identify the most optimal geometry for the hydrogels to induce shape morphing at the lowest possible strains and forces. Future work will consider the development of a fully integrated passive sensor prototype, with each end of the star pattern bonded with a hydrogel copolymer actuator. The radio frequency signatures of these passive wireless antenna sensors will be characterized as they shape morph in response to relevant environmental stimuli.

ACKNOWLEDGEMENTS

This work was supported by the U.S. Office of Naval Research (ONR) under grant no. N00014-22-1-2591.

REFERENCES

[1] Y. Park, G. Vella, and K. J. Loh, “Bio-Inspired Active Skins for Surface Morphing,” *Scientific Reports*, vol. 9, no. 1, Dec. 2019.

[2] L. Tang, L. Gong, G. Zhou, L. Liu, D. Zhang, J. Tang, and J. Zheng, “Design of Low Temperature-Responsive Hydrogels used as a Temperature Indicator,” *Polymer (Guildf)*, vol. 173, pp. 182–189, May 2019.

[3] D. Keskin, T. Mokabbar, Y. Pei, and P. van Rijn, “The Relationship between Bulk Silicone and Benzophenone-Initiated Hydrogel Coating Properties,” *Polymers 2018,* vol. 10, no. 5, p. 534, May 2018.

[4] B. A. Grzybowski, R. Haag, N. Bowden, and G. M. Whitesides, “Generation of Micrometer-Sized Patterns for Microanalytical Applications Using a Laser Direct-Write Method and Microcontact Printing,” *Annual Review of Materials Research*, vol. 37, no. 3, p. 6, 1998.

[5] H. Yuk, T. Zhang, G. A. Parada, X. Liu, and X. Zhao, “Skin-inspired hydrogel-elastomer hybrids with robust interfaces and functional microstructures,” *Nature Communications*, vol. 7, p. 12028, Jun. 2016.

[6] Y. Park and K. J. Loh, “Controlling 3D Deformations of Bio-Inspired Active Skins through Designed Geometrical Imperfections,” *Journal of Materials Science*, *under review*.